

Effect of hanging-type sand fence on characteristics of wind-sand flow fields

Jian-jun Cheng^{1,2}, Jia-qiang Lei^{*1}, Sheng-yu Li¹ and Hai-feng Wang¹

¹*Xinjiang Institute of Ecology and Geography, Chinese Academy of Sciences, Urumqi, Xinjiang, 830011, China*

²*College of Water Resources and Architectural Engineering, Shihezi University, Shihezi Xinjiang 832003, China*

(Received December 3, 2015, Revised March 30, 2016, Accepted April 6, 2016)

Abstract. A hanging-type sand-retaining wall is a very common sand-blocking fence structure used to prevent sand movement. This type of wall is widely used along the Qinghai–Tibet and Gobi desert railways in Xinjiang, Western China. To analyze the characteristics of wind-sand flow fields under the effect of such a sand fence structure, a wind tunnel test and a field test were carried out. The wind tunnel test showed the zoning characteristics of the flow fields under the effect of the hanging-type sand-retaining wall, and the field test provided the sediment transport data for effective wind-proof interval and the sand resistance data in the front and behind the sand-retaining wall. The consistency of the wind-sand flow fields with the spatial distribution characteristic of wind-carried sand motion was verified by the correspondences of the acceleration zone in the flow field and the negative elevation points of the percentage variations of the sand collection rate. The spatial distribution characteristic of the field sand collection data further showed the spatial structural characteristic of the sandy air currents under the action of the hanging-type sand-retaining wall and the sand resistance characteristic of the sand-retaining wall. This systematic study on the wind-sand flow fields under the control of the hanging-type sand-retaining wall provides a theoretical basis for the rational layout of sand control engineering systems and the efficient utilization of a hanging-type sand-retaining wall.

Keywords: wind-sand environment; wind-sand disaster; hanging-type sand-retaining wall; wind-sand flow fields; wind-blown sand prevention and control

1. Introduction

With the implementation of the “develop-the-west strategy” in China in the recent years, the plateau railway connecting the Qinghai province and Tibet autonomous region has been completed and under operation, along with the construction of the southern and northern Xinjiang railway network. This will lead to huge future developments. However, because of special geographic and climatic environment of these regions, the railway operation is inevitably subject to the problems of wind-sand movement and the need for its control. The Qinghai–Tibet plateau is a high-altitude and arid region because of long windy periods, sparse surface vegetation, and loose soil, and the

*Corresponding author, Professor, E-mail: desert@ms.xjb.ac.cn

Qinghai–Tibet railway constantly experiences wind-sand disasters (Cheng *et al.* 2014, Wang *et al.* 2007, Zhang *et al.* 2010, 2012). The railways in Xinjiang pass through well-known high wind areas such as Hundred Miles, Yan Dun, and Thirty Miles, without surface vegetation and containing coarse sand and gravel. When the wind is strong, because of the presence of sand, the passing trains can be damaged (Cheng *et al.* 2015). To guarantee the smooth running of the railways, massive systematic mechanical sand prevention engineering measures have been built along the Qinghai–Tibet and Gobi desert railways in Xinjiang. These measures on one hand satisfy the urgent need to overcome wind-sand disasters, and on the other hand overcome the difficulty or impossibility of building a vegetation-based sand prevention system in these regions. The mechanical sand prevention system is mainly composed of sand-blocking, sand-fixing, and sand-guiding engineering measures. The sand-blocking engineering measures are located at the forefront of the windward side of the entire system and perform the primary task of blocking passing sandy air currents. The sand-blocking engineering measures include the hanging-type sand-retaining wall, sleeper-type sand-retaining wall, and high vertical-type PE net sand fence. Among them, the hanging-type sand-retaining wall has been widely used in the engineering field because of its simple production process and convenient construction (Fig. 1).

The vortex zone and the laws of the flow field on the leeward side of a sand fence have been widely studied (Perara 1981, Cleugh and Hughes 2002). Lee Sang-Joon *et al.* (2002) studied the shelter effect of a holed-plank fence for sand drift on the leeward side of the sand fence using a wind tunnel test. Dong *et al.* (2006, 2007) determined the evolution pattern of the vortex zone on the leeward side of a vertically holed sand fence using a wind tunnel test. Although these studies cannot be directly used to guide the engineering of practical sand prevention, they nevertheless laid a foundation for the study of the sand prevention effects of concrete sand control engineering measures.

The hanging-type sand-retaining wall has been used as a common feature in the engineering practice of sand prevention for less than a decade. Therefore, there is a lack of systematic experimental and theoretical analysis and studies on its sand control effects and combined use with other engineering measures, because its application is still based on engineering experience. Therefore, in this study, taking the hanging-type sand-retaining wall as an example, a wind tunnel test was carried out to simulate the trend of flow fields, combined with a field test to completely determine the characteristics and laws of wind-sand flow fields under the effect of hanging-type sand-retaining wall. This will provide a theoretical basis for the design of sand control measures along the railways in normal deserts, specifically in the Gobi desert.

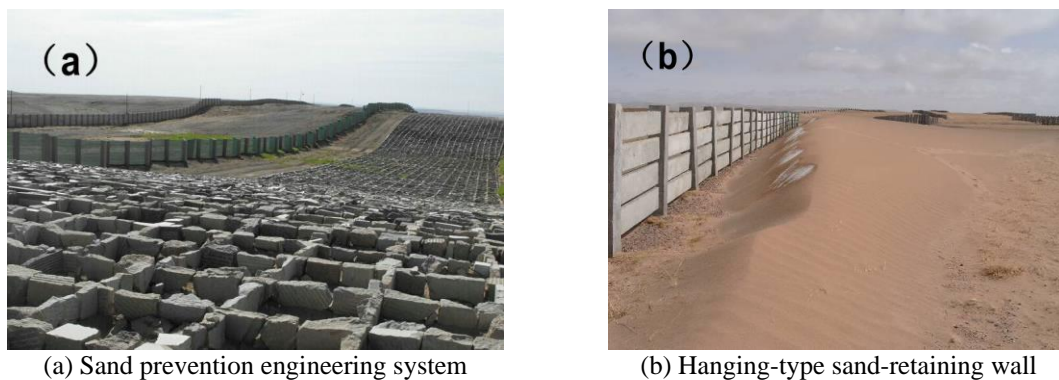


Fig. 1 Sand prevention systems and sand-blocking engineering measures along the railways

2. Experimental apparatus and methods

2.1 Wind tunnel test

The wind tunnel test was carried out using a unidirectional airflow environmental wind tunnel with a length of 16.2 m, consisting of a power section, test section, and diffusion section. The length of the test section was 8 m in length. The cross-sectional shape of the test section was a rectangle with 1.3 m width and 1 m height, and the thickness of the boundary layer of the wind tunnel was 15 cm (Fig. 2).

Fig. 3 shows the arrangement of the test model (10 cm in height). The scale of the model to the actual sand fence structure was 1:20. The test sections in the wind tunnel were set at a location of 0H (the location of the sand fence), 0.5H, 1H, 4H, 7H, and 10H on the windward side of the wind tunnel, and at -1H, -2H, -3H, -5H, -10H, -15H, and -20H on the leeward side, respectively. Considering that a certain effect of baseboard roughness on flow fields, bronzing raw emery paper was paved on the baseboard of the wind tunnel to increase its roughness. The wind speed monitoring points of the Pitot tube in the vertical direction were 1 cm, 2 cm, 3 cm, 5 cm, 7 cm, 10 cm, 15 cm, 30 cm, and 50 cm in height. Because of a relatively significant effect of the sand fence on the flow field on the leeward side, more monitoring points were provided on the leeward side during the wind tunnel test. The test was carried out under the given wind speed conditions, and the inflow wind speeds were set at 8 m/s, 10 m/s, 12 m/s, and 14 m/s, respectively. Before the sand fence model-based test, cavity flow field test without the arrangement of a sand fence model was carried out first for a comparative analysis of flow fields.

Besides using the wind tunnel test data for full-flow-field mapping calculation, the vertical wind speed profiles at different distances from the sand fence were also obtained for a comparative analysis of the wind speed variations along the fence. The wind-proof efficiency was calculated as follows

$$w_{ij} = \frac{(v_{nij} - v_{hij})}{v_{nij}} \times 100\% \quad (1)$$

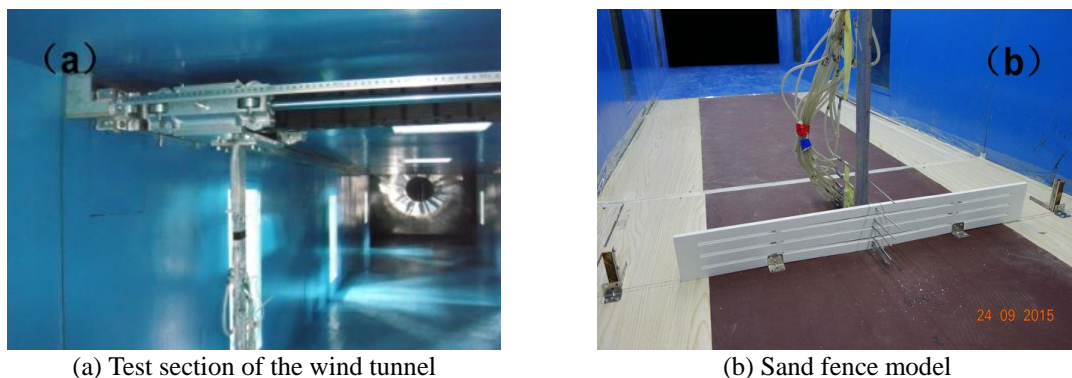


Fig. 2 Wind tunnel equipment and sand fence model

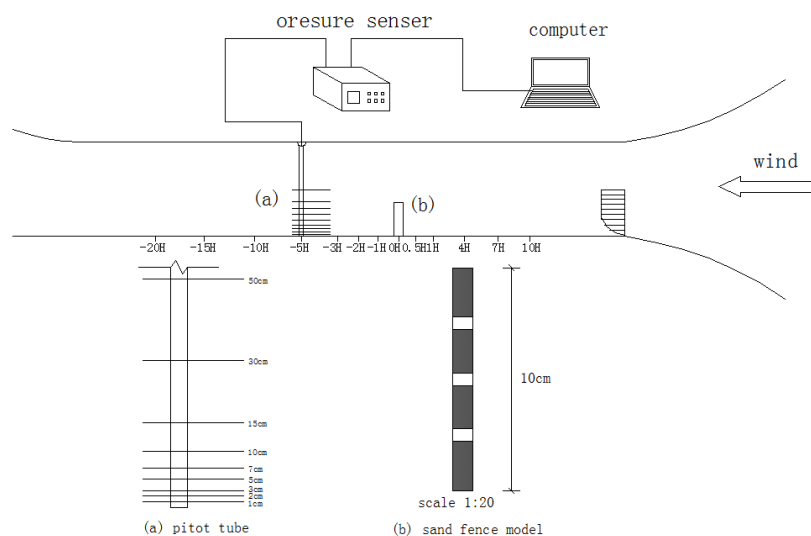


Fig. 3 Test principle of the wind tunnel test and the design drawing of the test section

where w_{ij} represents the wind-proof efficiency value (%) of the coordinate point (i, j) ; v_{nij} represents the wind speed value of the coordinate point (i, j) at a given wind speed and under the cavity field condition without a sand fence arrangement; v_{hij} represents the wind speed of the coordinate point (i, j) at a given wind speed and under the condition with a sand fence arrangement.

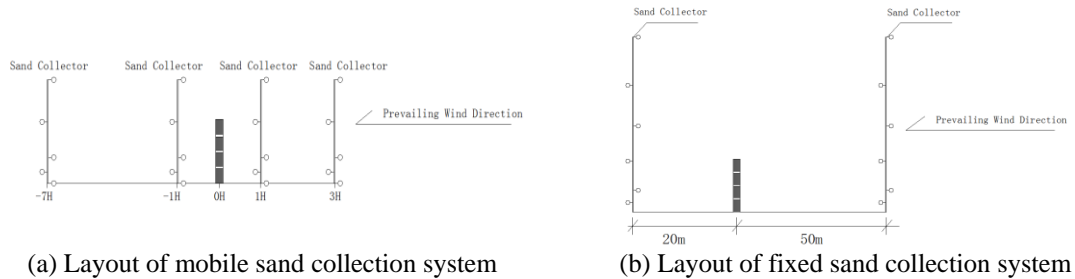
2.2 Field test

To determine the effect of hanging-type sand-retaining wall on the sediment transport and sand resistance characteristics, a field test was carried out along railway sections where the hanging-type sand-retaining wall had been erected. The field test consisted of two parts: the sediment transport characteristic in the effective wind-proof space of the retaining wall and the sand resistance characteristic of the sand-retaining wall.

The field test on the sediment transport was carried out using four sets of mobile gradient sand collection systems simultaneously, each with a height of 3 m, and rotary sand collection systems were installed at each of five elevation points (0 m, 0.5 m, 1 m, 2 m, and 3 m). Four sets of sand collection systems were laid out on the windward side of the sand-retaining wall (3H and 1H away from the wall) and on the leeward side of the sand-retaining wall (-1H and -7H away from the wall), as shown in the field layout (Fig. 4(a)). The sediment transport rate was tested with a strong wind for the duration, and the field average inflow wind speed of the test was about 10 m/s. The sediment transport rate of each monitoring point can be calculated using the following Formula.

$$Tr = m / s \cdot t \quad (2)$$

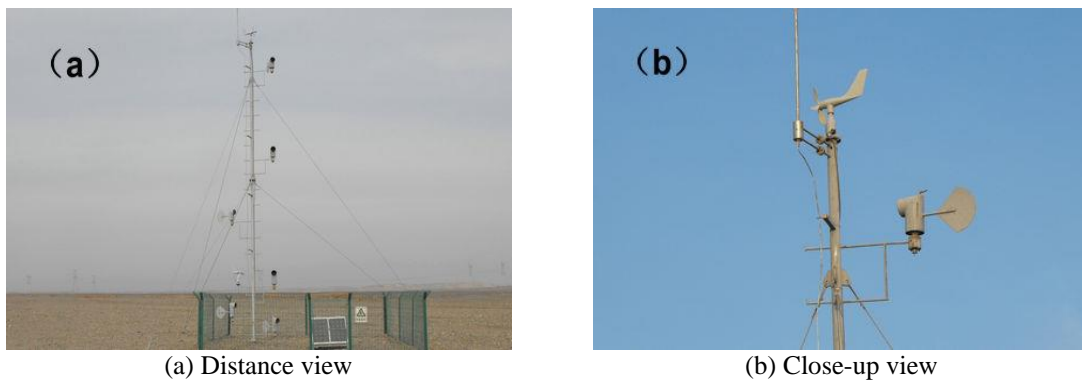
Where Tr represents the sand transport rate; m is the weight of the sand collected using a gradient sand sampler in g; s is the area (in cm^2) of the windward entrance of the sand sampler; t is the duration of the wind speed (in h) exceeding that of a sand-driving wind.



(a) Layout of mobile sand collection system

(b) Layout of fixed sand collection system

Fig. 4 Layout of sand collection systems used in field test



(a) Distance view

(b) Close-up view

Fig. 5 Sand collection system

The height of the main tower of the sand collection system used in the field test for the sand resistance characteristic of the sand-retaining wall was 10 m. Sand collectors were set at six elevation points (i.e., 0.5, 1, 2, 4, 6, and 9 m) in the sand collection test system (Fig. 5). The sand collectors had a round windward inlet with a diameter of 20 cm. The sand collection test system can automatically adjust the sand collection direction according to the wind direction. The sand collection data were collected every 30 days; on heavy wind days during the test period, the data were collected after a strong wind to prevent the sand collectors from overflowing and making the data invalid. After the data collection, laboratory soil tests were conducted to analyze the physical properties of the particulates and obtain the statistics of grain gradation, size composition, and other relevant data. The relative locations of the sand collection systems and inclined inserting-type sand fence are shown in Fig. 4b. One sand collection system was arranged on the windward side (50 m), and the other was arranged on the leeward side (20 m) of the sand fence. The sand collection data on the windward side represent the data of the original sandy air current, whereas those on the leeward side represent the data of the passing sandy air current that could not be retained by the sand fence. The difference between these two represents the data of the sandy air current retained by the sand fence. Besides analyzing the physical properties of the particulates, the data collected were also used to calculate the sand collection rate and the percent change in the sand collection rate.

The formula of sand collection rate can be expressed as follows

$$R_i = m_i / s \quad (3)$$

where R_i represents the sand collection rate of the i th sand collector (g/m^2); m_i represents the mass of the sand collected by the i th sand collector (g); s represents the windward mouth area of the sand collector, $s = \pi r^2$, $r = 10$ cm.

The percent change in the sand collection rate can be expressed as follows

$$\eta_i = \frac{R_{fi} - R_{bi}}{R_{fi}} \times 100\% \quad (4)$$

Where η_i represents the percent change in the sand collection rate of the i th sand collector (dimensionless); R_{fi} represents the sand collection rate corresponding to the i th sand collector of the sand collection system on the windward side (50 m) of the sand fence; R_{bi} represents the sand collection rate value corresponding to the i th sand collector of the sand collection system on the leeward side (20 m) of the sand fence.

The sand resistance rate can be expressed as follows

$$K = \frac{\sum_{i=1}^6 m_{fi} - \sum_{i=1}^6 m_{bi}}{\sum_{i=1}^6 m_{fi}} \times 100\% \quad (5)$$

K represents the sand resistance rate; m_{f1} , m_{f2} , m_{f3} , m_{f4} , m_{f5} , and m_{f6} represent the sand collection data collected by sand collectors at the six heights (0.5, 1, 2, 4, 6, and 9 m, respectively) of the sand collection system on the windward side (50 m) of the sand fence; m_{b1} , m_{b2} , m_{b3} , m_{b4} , m_{b5} , and m_{b6} , represent the sand collection data collected by sand collectors at the six heights (0.5, 1, 2, 4, 6, and 9 m, respectively) of the sand collection system on the leeward side (20 m) of the sand fence. The value of the sand resistance rate represents the reduction percent of the sandy air current on the full section perpendicular to the passing sandy air current.

3 Results

3.1 Flow field characteristics under effect of sand-retaining wall

3.1.1 Trend of flow fields

Fig. 6 shows the form of the inflow wind speed profile when it is unaffected by the sand fence. Generally, the flow field formed without the sand fence is relatively smooth; however, under the effect of the hanging-type sand-retaining wall, the smoothness of the flow field is completely disturbed (Fig. 7). In the flow field, a deceleration zone in front of the wall, an acceleration zone behind the wall, and a vortex zone behind the wall appeared successively, and the acceleration zone was located above the vortex zone, wrapped by the deceleration zone outside.

The deceleration zone in front of the sand-retaining wall is the deceleration phenomenon of the air current congestion effect of the flowing air current when encountering the sand-retaining wall.

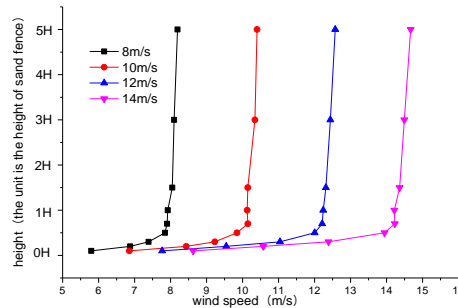


Fig. 6 Inflow wind speed profile at the entrance

The figure shows that the air current congestion started at 5H in front of the wall and gradually enhanced until it reached the sand-retaining wall. At the location of the sand-retaining wall, because of the transverse gaping characteristic, the air current accelerated when passing through the seams, but the accelerated current then diffused after passing through the seam pores of the planks, resulting in a non-uniform distribution of the current velocity in the vortex zone behind the wall.

Therefore, the influence region of the holes on the slab joint on the vortex zone at the leeward side of the wind was within the vortex zone. With an increase in the inflow wind velocity, the deceleration effect in front of the sand-retaining wall was weakened, the acceleration effect in the acceleration zone above the leeward side of the sand-retaining wall was further improved, and the range of the vortex zone behind the sand-retaining wall was expanded; however, the deceleration degree in the vortex zone was weakened. The acceleration zone in the vertical direction started from a distance of 3H, and the distance of 4H was the core area of the acceleration zone. When the inflow wind speed was 8 m/s, the deceleration-influenced distance on the leeward side of the sand-retaining wall can reach to 1H. When the wind speed increased to 14 m/s, the deceleration-influenced distance can reach to 1.5H.

3.1.2 Characteristics of wind speed profiles

To further analyze the effects and trend of the hanging-type sand-retaining wall on the entire speed field, six typical locations: 4H, 1H, 0H, -1H, -4H, and -20H, were selected successively in the front and behind the sand-retaining wall (where H represents the height of the sand-retaining wall, and “-” represents the leeward side), for a comparative analysis of the trend of the wind speed profile along the way. As shown in Fig. 8, under specific wind speed conditions, the form of the wind speed profile along the way changed intensely from 4H away from the wall on the windward side of the sand-retaining wall to -20H away from the wall on the leeward side of the sand-retaining wall. The wind speed profile at 4H away from the wall on the windward side of the sand-retaining wall was affected by the flow resistance of the wall, and the wind speed profile at this site varied slightly in scope at a distance of greater than 1H. However, when closer than 1H, sudden variation points in the wind speed were observed. For the variation characteristic of the wind speed profile at 1H away from the wall on the windward side of the sand-retaining wall relative to the form of the inflow profile at the entrance, the wind speed of the upper section of the wind speed profile curve (>1H) increased, while the wind speed of the lower section (<1H)

decreased. At OH, where the sand-retaining wall was located, the wind speed profile varied intensely in the horizontal direction. Below 1H, the wind speed at the seam pore of the plank was relatively high, and the wind speed values for other points were close to 0.

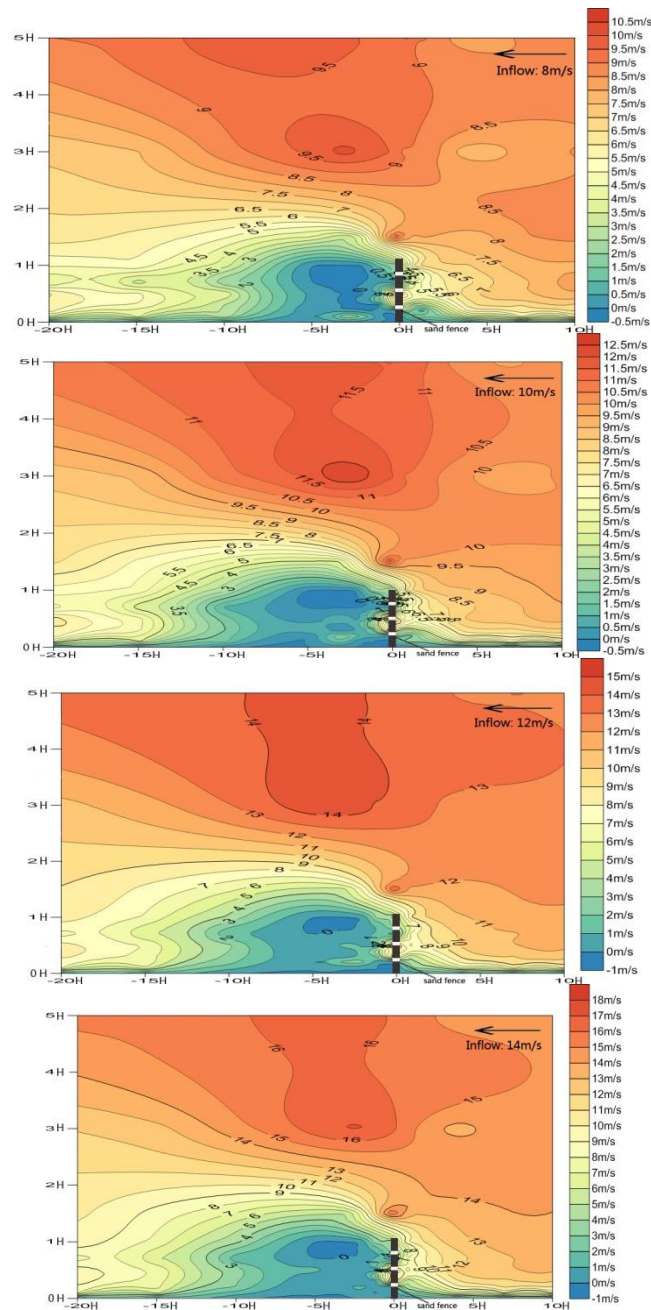


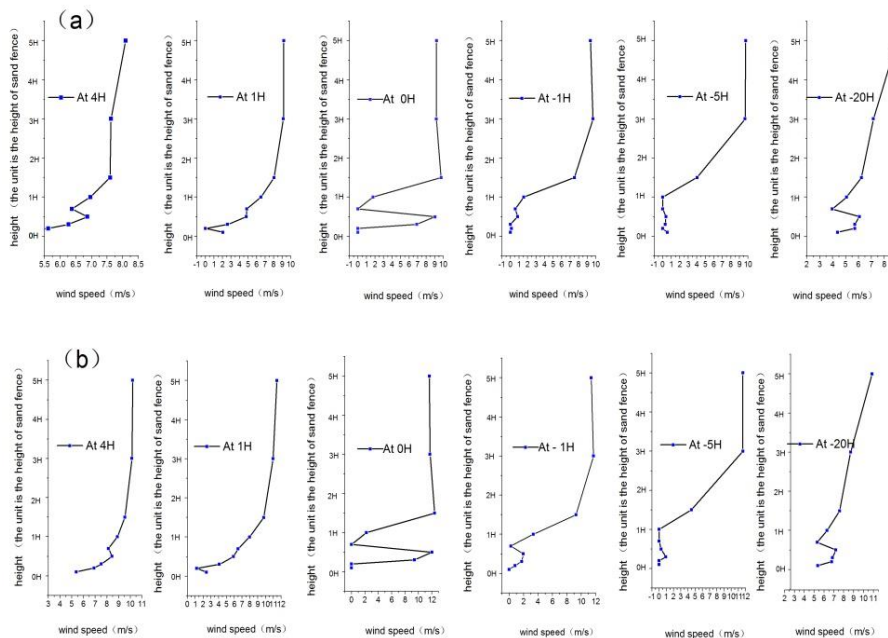
Fig. 7 Flow field evolution of hanging-type sand-retaining wall

However, at distances greater than the wall height (1H), the wind speed varied relatively slightly. At $-1H$ and $-5H$ away from the wall on the leeward side of the sand-retaining wall, the wind speed profile for $<1H$ decreased sharply, and that greater than the sand fence height increased. At $-20H$ away from the wall on the leeward side of the sand-retaining wall, compared to the form of the inflow wind speed profile at the entrance, the variation in the wind speed profile was no longer significant, and instead presented a trend of gradually recovering the form of the inflow profile curve.

When the inflow wind speed at the entrance increased gradually from 8 m/s to 14 m/s, the trends and patterns of the wind speed profiles in front of and behind the sand-retaining wall were similar. This indicates a corresponding relationship between the penetration characteristic of the openings of the sand-retaining wall and the form of the wind speed profile, and the trend of the wind speed profile is not restricted by the wind speed of the inflow air.

3.1.3 Wind-proof efficiency

Considering that the actual design height of the hanging-type sand-retaining wall is about 2 m, three characteristic heights (0.1H, 1H, and 5H) were selected in the vertical direction to calculate the wind-proof efficiency of the hanging-type sand-retaining wall using Formula (1). 0.1H was the upper-limit height of the wind-sand flow movement in the form of creep; 1H was the upper-limit height of the wind-sand flow movement mainly in the form of saltation; 5H was the height of the wind-sand flow when moving by flying. When the inflow wind speed decreased to ~ 6 m/s, the effective deceleration was reached, as 6 m/s was the critical wind speed of sand-blowing. When the inflow wind speed was 8 m/s and the sand control efficiency was 25%, the effective deceleration could be reached.



Continued-

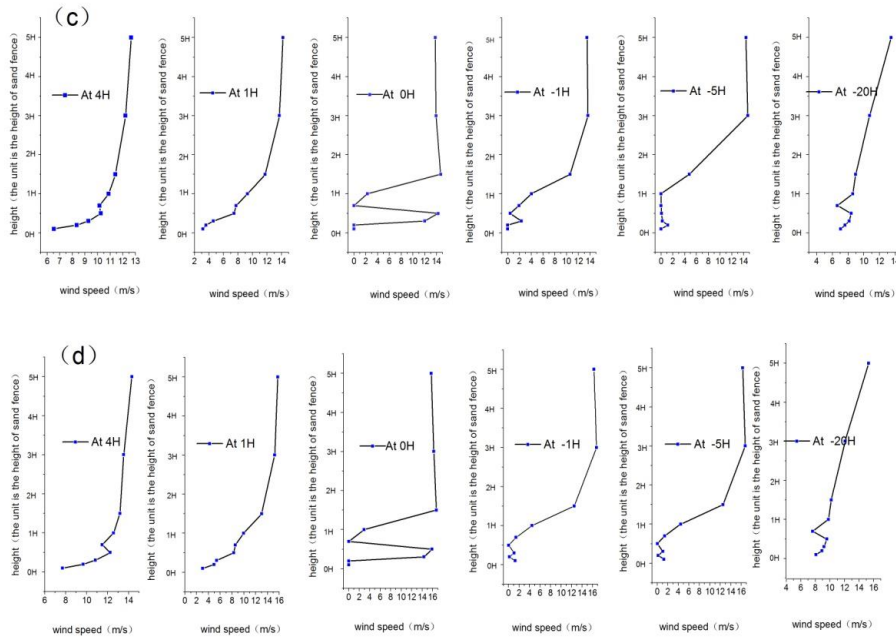
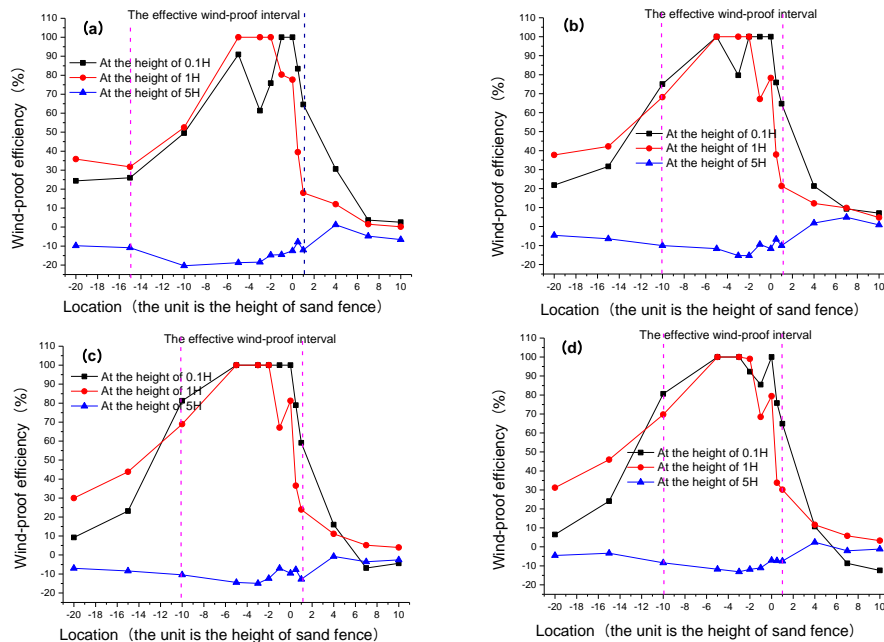


Fig. 8 Evolution curves of wind speed profile (a) Inflow: 8 m/s, (b) Inflow: 10 m/s, (c) Inflow: 12 m/s and (d) Inflow: 14 m/s



(a) Wind speed: 8 m/s (b) Wind speed: 10 m/s (c) Wind speed: 12 m/s. (d) Wind speed: 14 m/s

Fig. 9 Wind-proof efficiency of hanging-type sand-retaining wall

Thus, for an inflow wind speed of 8 m/s, the effective wind-proof interval started from $-15H$ away from the wall on the leeward side of the sand-retaining wall. When the inflow wind speeds were 10 m/s, 12 m/s, or 14 m/s, the effective wind-proof interval started from $-10H$ away from the wall on the leeward side of the sand-retaining wall. Fig. 9 shows that within the effective wind-proof region, only the wind speeds at the elevation points of $0.1H$ and $1H$ were decelerated, and the deceleration effect was poor regarding the wind speed at an elevation point of $5H$. That is, the hanging-type sand-retaining wall significantly affected the sandy air currents in motion in the forms of creep and saltation, but could not retain passing sandy air currents that were flying.

3.2 Law of sand control by sand-retaining wall

The trend of sand control by the hanging-type sand-retaining wall was studied from two aspects: the trend of the spatial sediment transport rate in the effective wind-proof interval and the trend of sand resistance regarding sandy air currents under the effect of the sand-retaining wall.

3.2.1 Spatial sediment transport characteristic in effective wind-proof interval

Clearly, in an effective wind-proof interval, the variation in the sediment transport rates at the sites at different distances away from the sand-retaining wall are similar. Below the height of 1 m, the sediment transport rates decreased with an increase in the height, and among them, the vertical sediment transport rate at $1H$ away from the wall on the windward side of the sand-retaining wall decreased continuously with an increase in the height.

The vertical sediment transport rate characteristics at $3H$ away from the wall on the windward side of the sand-retaining wall and at $1H$ and $7H$ away from the wall on the leeward side of the sand-retaining wall were similar, i.e., the sediment transport rates at a height of 2 m were higher than those at a height of 1 m. At a height of 3 m, the sediment transport rates of all the sites were close to 0. This can be attributed to the inflow wind speed of the field test. In the field test, the inflow wind speed was about 10 m/s, the motion of wind-carried sand was dominated by creep and saltation, and the flying height of the fine sand particulates was relatively low (Fig. 10).

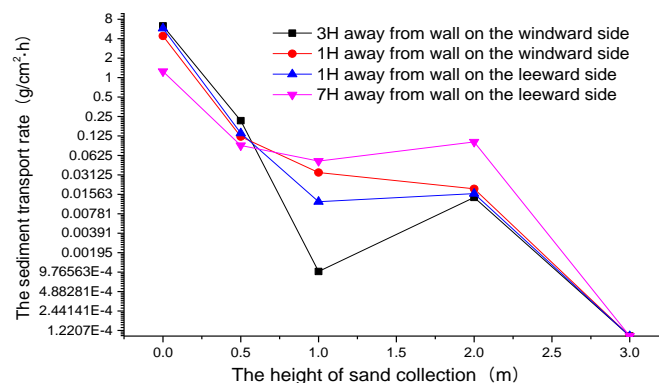


Fig. 10 Sediment transport rate characteristic in effective wind-proof interval

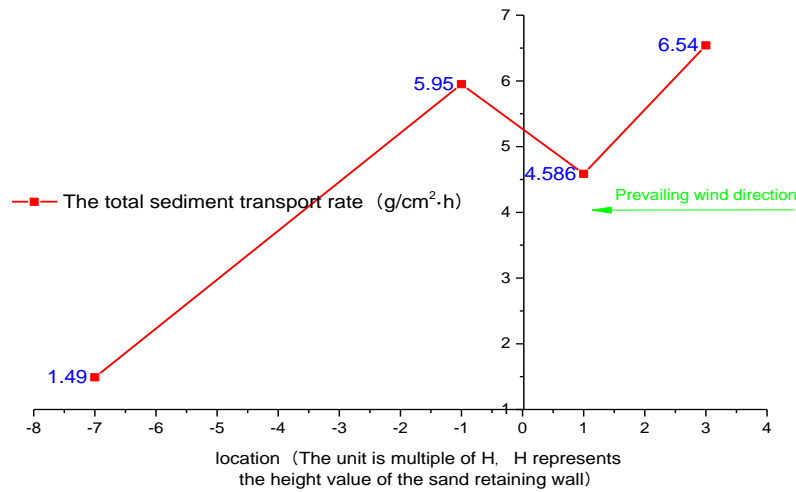
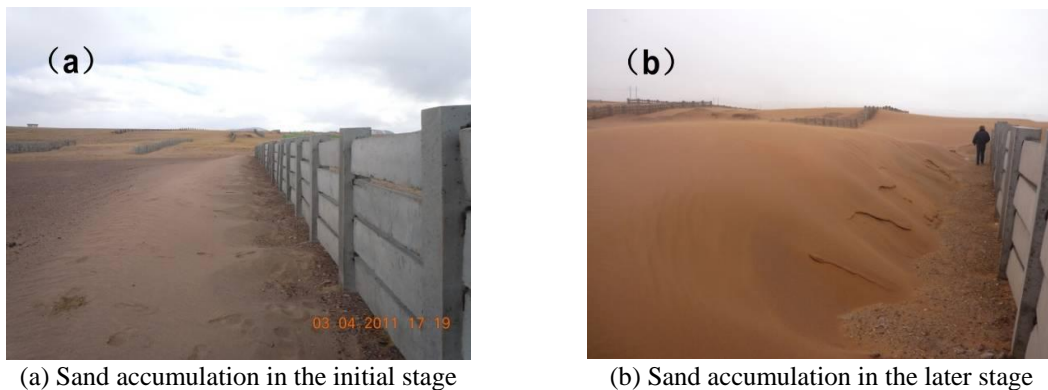


Fig. 11 Sectional total sediment transport rate in effective wind-proof interval



(a) Sand accumulation in the initial stage

(b) Sand accumulation in the later stage

Fig. 12 Forms of sand accumulation on the leeward side of hanging-type sand-retaining wall

Fig. 11 shows the variation curve along the total sediment transport at sites at different distances away from the sand-retaining wall on the windward side. This shows that the total sediment transport rate at $3H$ away from the wall on the windward side of the sand-retaining wall was the highest. When the sandy air currents moved to $1H$ in front of the sand-retaining wall, the sediment transport rate decreased abruptly as a result of the air current congestion effect in front of the wall on the exposed side of the sand-retaining wall. The sediment transport rate at $1H$ away from the wall on the leeward side of the sand-retaining wall showed an increasing trend than that on the windward side. This is because the process at $1H$ away from the wall on the leeward side of the sand-retaining wall was the transition process of the currents passing through the seam pores of the planks from acceleration to dispersion behind the wall, and it was also the process of the deposition of sand particulates towards the leeward side after bypassing the top of the wall through the windward side of the sand-retaining wall. This characteristic was also reflected in the form of

the sand accumulation on the leeward side of the sand-retaining wall (Fig. 12). No sand deposition or accumulation occurred within 1H of the wall on the leeward side of the sand-retaining wall, and the sand accumulation gradually increased beyond 1H. This also indicated the complexity of the sandy air current motion in the vortex zone on the leeward side of the sand-retaining wall. When the motion of the wind-carried sand reached 7H away from the wall on the leeward side of the sand-retaining wall, the sand carried by the wind was largely deposited due to the deceleration in the vortex zone on the leeward side of the sand-retaining wall. The deposition amount from the sandy air currents passing 7H was relatively small; therefore, the sediment transport was relatively small as well.

3.2.2 Spatial sand collection characteristic in front of and behind sand-retaining wall

The sand collection data at various distances from the sand collection system in front of and behind the hanging-type sand-retaining wall erected in the “Yan Dun” section along the Lanxin High-Speed Railway II in Xinjiang can be calculated using Formula (3). The data collected by the sand collection system 50 m away from the wall on the windward side of the sand-retaining wall showed the characteristics of the original sandy air current; the data collected by the sand collection system 20 m away from the wall on the leeward side of the sand-retaining wall showed the characteristics of the sandy air current that had not been retained by the sand resistance effect of the sand-retaining wall. Fig.13 shows that the sand collection rates in front of and behind the sand-retaining wall both had a power exponential decline curve with an increase in distance. Differences were observed between the sand collection rates in front of and behind the sand-retaining wall starting with a distance of 4 m, and this increased as the distance decreased.

Fig. 13 shows the spatial distribution characteristics of the percentage variations in the sand collection rates in front of and behind the sand-retaining wall. This shows that the percentage variations in the sand collection rates in front of and behind the sand-retaining wall approached 50% at a distance of 0.5 m (i.e., almost half of the sand particulates were retained), and that the percentage variations in the sand collection rates decreased as the distance increased. At 4 m, the percentage variations in the sand collection rates reached 12.86%, indicating that with a height of only 2 m, the sand-retaining wall can still retain the passing sandy air currents to a certain extent. At 6 m, the percentage variations in the sand collection rates became negative (Fig. 14), indicating that the amount of the sand particulates carried by the wind at this distance increased instead, and the sand flux per unit area at this distance increased under the effect of the sand-retaining wall. This seems difficult to explain, but when combined with the flow field diagram of the sand-retaining wall, the emergence of the negative values becomes rational, as there was an acceleration zone at 3H from the leeward side of the sand-retaining wall, and an increase in wind speed would inevitably increase the sand flux per unit area.

3.2.3 Spatial characteristics of size composition and grain gradation of sand collection

The motion of the wind-carried sand has a stratification characteristic in the vertical direction: Under the effect of gravity, the larger sand particulates usually move to lower layers, whereas the smaller particles usually move to the upper layers. When the motion of the wind-carried sand encounters the sand fence, the change in the wind-sand flow field, on one hand, changes the mass of the passing sand per unit area at each height and, on the other hand, changes the grain gradation at each height.

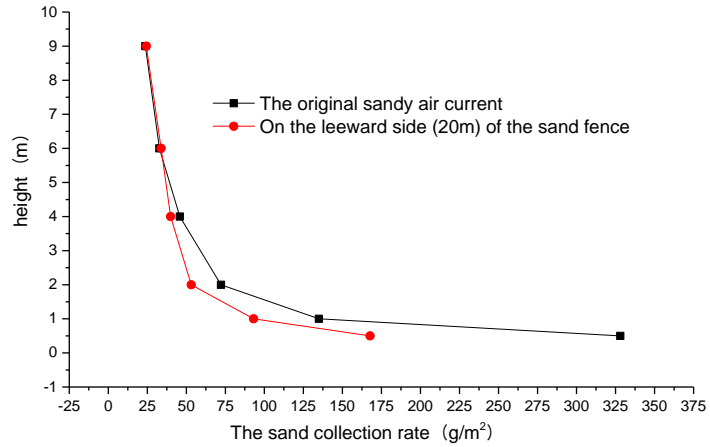


Fig. 13 Gradient distribution characteristic of sand collection in front of and behind sand-retaining wall

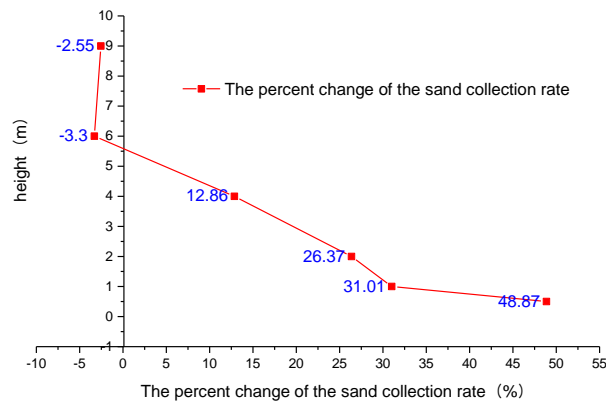


Fig. 14 Percentage variations in sand collection rate for sand-retaining wall

Table 1 Amounts of sand collected at various elevation points of sand collection system

Collection location	Collection elevation (m)					
	0.5	1.0	2.0	4.0	6.0	9.0
Amount of sand collected on windward side mf (g)	103.01	42.37	22.68	14.39	10.29	7.46
Amount of sand collected on leeward side mb (g)	52.67	29.23	16.70	12.54	10.63	7.65

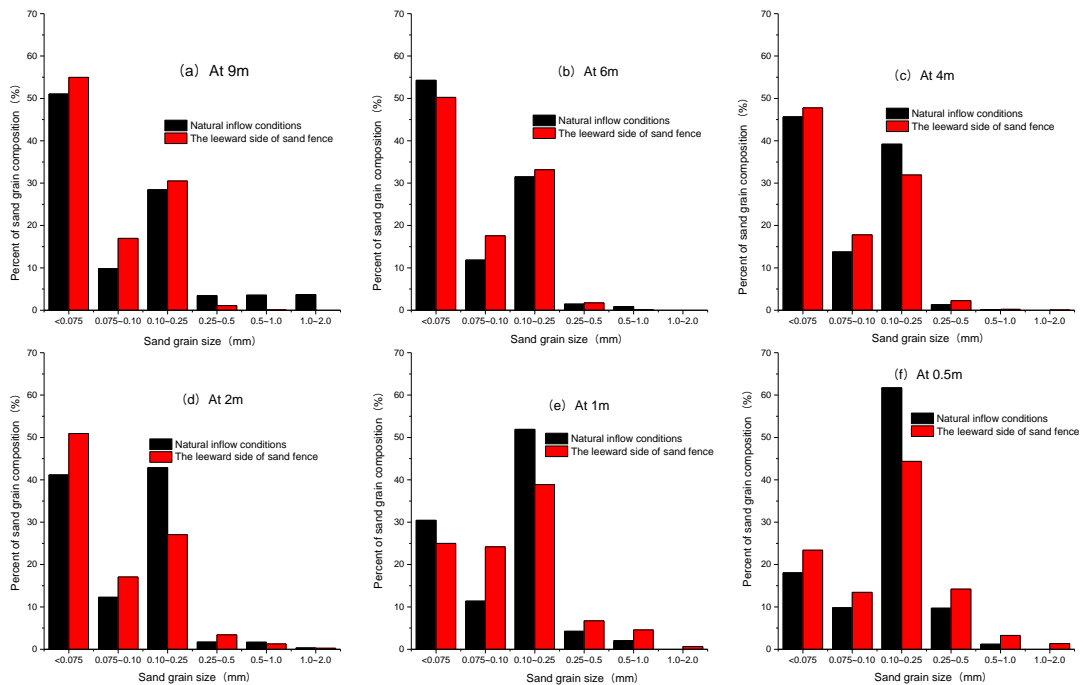


Fig. 15 Size distribution characteristics of vertical gradient sand collection in front of and behind sand-retaining wall

As shown in Fig. 15, compared to the size composition of the sandy air current under the natural inflow conditions, the size composition of the sandy air current that passed through the sand fence underwent some changes: At 9 m, there was a lack of sand particulates above 0.5 mm in size, whereas the percentage of those below 0.25 mm increased significantly. At 6 m and 4 m, the size composition after passing through the sand fence was close to that under the natural inflow conditions, indicating that the sandy air current motion did not change the grain gradation relation owing to the effect of the sand fence at these points. At 2 m, 1 m, and 0.5 m, a common characteristic was that the sand particulates with a medium size, i.e., within the size range 0.1–0.25 mm, had a significantly reduced percentage after passing through the sand fence; whereas those in the other size composition ranges had increased percentages after passing through the sand fence.

To sum up the abovementioned trend, under the flow disturbance effect of the sand-retaining wall, the large particulates (size >0.25 mm) in the high-altitude suspension were forced to be deposited. In the range below the height of the sand-retaining wall (2 m), a common characteristic among the various elevation points was that the percentage of the sand particulates within the medium size range (0.1–0.25 mm) decreased significantly, and the lower the elevation point, the more significant the decrease. Moreover, an increasing trend was observed in the percentages of sand particulates within the other size ranges.

3.2.4 Calculation of sand-blocking rate of sand-retaining wall

The sand-blocking rate of the sand-retaining wall can be calculated using the sand collection data from in front of and behind the hanging-type sand-retaining wall in the Yan Dun section along the Lanxin high-speed railway II.

After substituting the data for various elevation points in Table 1 into Formula (5), the sand-blocking rate was $K=37,85\%$. That is, the hanging-type sand-retaining wall had an average sand-blocking rate of 37.85%. Among the sand control engineering systems laid out along the railways, the hanging-type sand-retaining wall only represents one type, and the sand-blocking engineering measures usually need to be combined with sand-fixing engineering measures before they can maximally control the harm done by the passing drift of sand to the railways.

4. Conclusions

- As shown by the wind tunnel test, under the effect of the hanging-type sand-retaining wall, the flow field can be divided into congestion deceleration zone, acceleration zone, and vortex deceleration zone.
- As indicated by the calculated wind-proof efficiency, the minimum effective wind-proof interval of the hanging-type sand-retaining wall ranged from $-10H$ on the leeward side of the sand-retaining wall to $1H$ on the windward side with an influencing distance of $11H$. When the actual height of the sand-retaining wall was 2 m, the effective influencing range on the leeward side of the sand-retaining wall was 20 m, whereas that on the windward side of the sand-retaining wall was 2 m. In this interval, in the range below $1H$, a moderate average wind-proof efficiency was obtained; at a distance of $5H$, the wind-proof efficiency was relatively poor. In other words, the hanging-type sand-retaining wall had a satisfactory retention effect for the sand drift carried by the creep and saltation processes, but had no prevention or control effect for the flying fine particulates.
- As shown by the field sand collection test data, the sand-blocking rate of the sand-retaining wall showed a decreasing trend with increasing distance; at 6 m, the sand collection rate on the leeward side of the sand-retaining wall even exceeded that under natural inflow conditions on the windward side of the sand-retaining wall, indicating that the amount of sand carried by the air current per unit area at this distance increased instead of decreasing after passing through the sand-retaining wall. According to the flow field diagram, an acceleration zone existed at a distance $3H$ from the leeward side of the sand-retaining wall, and an increase in the wind speed increased the amount of sand carried, thus verifying the consistency of the wind-sand flow fields.
- The sand collection rates of the sand collectors were arranged vertical, on one hand showed the characteristics of the sandy air current structure in this region, and on the other hand, showed the temporal/spatial distribution characteristics of the sandy air current motion. After the motion of the wind-carried sand was subjected to the effect of the sand-retaining wall, the grain gradation changed at each height. Under the action of the plank seam-type sand-retaining wall, the amount of medium and coarse sand particulates in the sandy air currents decreased significantly, and because of the deposition of the coarse sand particulates on the leeward side of the wall after subjecting to the effect of the sand-retaining wall, the percentage of the fine sand particulates increased to a certain extent.

Acknowledgments

This research was supported by the National Natural Sciences Foundation of China (51568057, 51268050, 50908152). The authors also thank the reviewers and editors who helped to improve the quality of this paper.

References

- Bagnold, R.A. (1941), *The physics of blown sand and desert dunes*, Chapman & Hall, London.
- Cheng, J.J. and Xue, C.X. (2014), "The sand-damage-prevention Engineering System for the Railway in the Desert Region of the Qinghai-Tibet Plateau", *J. Wind Eng. Ind. Aerod.*, **125**, 30-37
- Cheng, J.J., Jiang, F.Q., Xue, C.X., Xin, G.W., Li, K.C. and Yang, Y.H. (2015), "Characteristics of the disastrous wind-sand environment along railways in the Gobi area of Xinjiang China", *Atmos. Environ.*, **102**, 344-354.
- Cheng, J.J., Jiang, F.Q., Yang, Y.H. and Xue, C.X. (2010), "Study on the hazard characteristics of the drifting sand along the railway in Gobi area and the efficacy of the control engineering measures", *China Railway Sci.*, **31**(5), 15-20.
- Cleugh, H.A. and Hughes, D.E. (2002), "Impact of shelter on crop microclimates: a synthesis of results from wind tunnel and field experiments", *Aust. J. Exp. Agric.*, **42**, 679-701.
- Dong, Z., Luo, W., Qian, G. and Wang, H. (2007), "A wind tunnel simulation of the mean velocity fields behind upright porous fences", *Agric. For. Meteorol.*, **146**, 82-93.
- Dong, Z., Qian, G., Luo, W. and Wang, H. (2006), "Threshold velocity for wind erosion: the effects of porous fences", *Environ. Geol.*, **51**, 471-475.
- Lee, S.J. and Lim, H.C. (2001), "A numerical study on flow around a triangular prism located behind a porous fence", *Fluid Dyn. Res.*, **28**, 209-221..
- Lee, S.J., Park, K.C. and Park, C.W. (2002), "Wind tunnel observations about the shelter effect of porous fences on the sand particle movements", *Atmos. Environ.*, **36**, 1453-1463.
- Lee, S.J., Park, K.C. and Park, C.W. (2002), "Wind tunnel observations about the shelter effect of porous fences on the sand particle movements", *Atmos. Environ.*, **36**, 1453-1463.
- Packwood, A.R. (2000), "Flow through porous fences in thick boundary layers: comparisons between laboratory and numerical experiments", *J. Wind Eng. Ind. Aerod.*, **88**, 75-90.
- Patton, E.G., Shaw, R.H., Judd, M.J. and Raupach, M.R. (1998), "Large-eddy simulation of windbreak flow", *Bound.-Lay. Meteorol.*, **87**, 275-307.
- Perera, M. (1981), "Shelter behind two-dimensional solid and porous fences", *J. Wind Eng. Ind. Aerod.*, **8**, 93-104.
- Wang, X.L., Zhang, D.X., Jiang, Y.H., Jiang, F.Q. and Li, Y. (2007), "Drifting sand disasters and engineering control along south Xinjiang railway line", *Chin. J. Geol. Hazard Control*, **18**(1), 59-63.
- Zhang, K.C., Qu, J.J., Han, Q.J. and An, Z.S. (2012), "Wind energy environments and Aeolian sand characteristics along the Qinghai-Tibet Railway", *China. Sedimentary Geology*, **273**, 91-96.
- Zhang, K.C., Qu, J.J., Liao, K.T., Niu, Q.H. and Han, Q.J. (2010), "Damage by windblown sand and its control along Qinghai-Tibet Railway in China", *Aeolian Res.*, **2**, 143-146.